Bull Eng Geol Environ (2018) 77:127–139
https://doi.org/10.1007/s10064-016-0951-x

ORIGINAL PAPER

Identifying the influences of geological factors on reservoir bank collapse by a model test

Feng Ji[1] · Changjiang Liu[1] · Huixing Zhou[2] · Haiming Liu[1] · Yi Liao[1]

Received: 12 May 2016 / Accepted: 1 October 2016 / Published online: 22 October 2016

Abstract Reservoir bank collapse, which strongly influences the relocation area when water is impounded, is currently an important topic in reservoir engineering. In this work, a series of orthogonal experiments was carried out to analyze, from among the many factors that can affect bank collapse width (BCW), the effects on BCW of slope angle, material grain-size diameter, degree of density of material, wave height of reservoir water, and water level fluctuation. A detailed analysis of each parameter is presented, and the analysis of range (ANORA) calculated. The results of the study show that the most sensitive factor affecting BCW is slope angle, followed by density degree, clay proportion, wave height, and water level. Finally, a prediction formula was established based on the physical simulation experiments, and its scope of applicability is discussed. These research results provide a reliable basis for future bank collapse studies.

Keywords Gravelly soil · Reservoir · Bank collapse · Physical simulation · Geological conditions

Introduction

With the rapid increase in human activities, an increasing number of geological hazards are occurring all over the world. After reservoir impoundment, the hydrological conditions of bank slopes are changed, which increases the risk of bank collapse (Kapayxev 1958; Andrew et al. 2000; Couper and Maddock 2001; Dapporto et al. 2003), and the topic of reservoir bank collapse has received considerable attention from many scholars.

The main approaches for forecasting bank collapse include empirical methods and statistical methods. The first important empirical formulae were presented by Kachugin (1949), who proposed the calculation formula of reservoir bank destruction forecasting, and Kondratjev (1956), who discussed the influence of wave depth. As for statistical methods, Mosselman et al. (2000) carried out a study on effect evaluation of bank stabilization on bend scour in anabranches of braided rivers. After investigating bank collapses of tens of reservoirs for nearly 10 years, Wang et al. (2000) proposed a "two-section method" and applied it to the prediction of bank collapses along the Waiyang–Fuzhou Railway Line. Xu (2003) also explored bank collapse and constructively raised arguments about the modification of the graphical method of bank collapse prediction in red rock areas on the basis of his research on redbed river valley slopes in the Sichuan Basin. Ma et al. (2002) and Fan et al. (2002) recommended the "analogy method with stable slide shape" in light of the principles of analogy in engineering geology. Tang et al. (2006a) and Xu et al. (2007) proposed a new method to predict bank collapse of the Three Gorges Reservoir Area called the Bank-Slope Structure Prediction Method (BSSPM). Malik and Matyja (2008) attempted to reconstruct bank erosion history by examining the anatomical changes in exposed tree roots. Regarding the different types of bank collapse, Zhang et al. (2002) categorized bank rebuilding into bank scour, whole slip, and rock mass collapse types, after analyzing the characteristics of the bank collapses at Fengjie in the Three Gorges Reservoir Area. Tang (2003)

✉ Changjiang Liu
65341207@qq.com

[1] State Key Laboratory of Geohazard Prevention and Geoenvironment Protection (Chengdu University of Technology), Chengdu 610059, People's Republic of China

[2] China Hydropower Consulting Grp Co, East China Investigat and Design Inst, Fuzhou, People's Republic of China

and Yin (2004) also made simple taxonomic studies of reservoir bank collapses. On the other hand, many scholars (Yao et al. 2011; Guan et al. 2011; Shu et al. 2012; Yu et al. 2015) studied the bank collapse process from the mutual exchange aspect between hydrodynamics and bank slope. Ta (2008) analyzed the long-term morphodynamic changes of the Yellow River through long sequence data. Furthermore, Wu (2014) simulated this process through experimental testing.

There are several existing methods of presenting the bank destruction approach. However, due to the complexity and uncertainty of bank collapse, there is always a deviation between forecasting results and actual practice, especially for the coarse-grained banks in the mountainous canyons of southwest China. For example, in the three typically researched reservoirs of the Dadu River, the accuracy of prediction was less than 60 % (Table 1).

Bank collapse is a progressive process. Thus, aside from the graphical and analogy methods, which are carried out by summarizing similar cases in other reservoirs that already have experienced bank collapse after a long history of water storage, another important method is to conduct modeling tests (physical modeling for bank collapse). This method is very important for discovering the mechanism of bank collapse, and for understanding the effect of a key factor. In the past, such experiments were primarily performed to simulate specific bank collapse, but some were used for sensitivity analysis. For example, Tang et al. (2006b) and Xu et al. (2007) conducted a sensitivity analysis in the Three Gorges Reservoir. It can be concluded from the multi-factor model test that the bank height, slope angle, constrained material size, and intensity of rainfall affects bank collapse, with slope angle playing the most important role of these four factors. The loss of volume on slopes and slope angle are directly related, and when one of the factors exceeds a certain limit, bank collapse occurs.

There are four factors in the previous experiments, excluding density degree, which we believe is an important factor from our long-term field investigations. As a result, five important factors were considered in this experiment, and the number of experimental groups increased to nine, which is more than ever before. On the basis of a previous study, we analyzed the factors influencing bank collapse width (BCW). Combined with lengthy field investigations, we selected five factors: slope angle, material diameter, water level, wave height of reservoir water, and density degree. Then, we performed a series of orthogonal experiments based on observed model deformation and destruction under different combinations, analyzing the mechanisms and regularity of the various factors affecting bank collapse. This work provides a reliable preliminary basis for model building and weight distribution.

Sample preparation and test methods

Experimental instrument

The facilities of the modeling test were all designed by the State Key Laboratory of Geo-hazards Prevention and Protection of China (Fig. 1). The modeling test system included two main simulation systems: the reservoir water storage model, and the rainfall simulation model. The reservoir water storage model included a manually adjusted testing flume with a length of 2 m, width of 1.5 m, and height of 0.6 m, and some other equipment that could also be adjusted manually for measuring displacement, water level, and pore-water pressure. The rainfall simulation model included circuit-checking systems for several pore-water pressures and overlapping insufflations simulating a rainfall system. All the data settings and collections were controlled by computers; waves were produced using the wave equipment (DC50 W-80), and wave height could be adjusted using the gear, reaching a maximum height of 0.04 m.

Table 1 Comparison of bank collapse width (BCW) prediction results with actual results of parts of a reservoir[a]

Reservoir	Water storage year	Typical profile position	Material composition	Predicted BCW (m)	Actual BCW (m)	Degree of accuracy (%)
Ertan reservoir	1998	Matoutian	Gravelly soil	60.5	35	58 %
		Daniuwan	Breakstone and gravelly soil	59.8	12	33 %
		Bawangshan	Silty clay containing breakstone	36.1	6.8	19 %
Baozhusi Reservoir	1996	Huangniliang	Silty clay containing breakstone	45.7	13	28 %
Gongzui Reservoir	1971	Zhusihe	Silty clay containing breakstone	33	0.5	2 %
		D06 segment	gravel-cobble soil	4.3	8	–
		D12 segment	gravelly soil	5.9	0.8	14 %

[a] These data were summarized by Tang et al. (2006a); the predicted BCW was calculated using Kachugin's graphical method, and the actual BCW was obtained through actual investigation

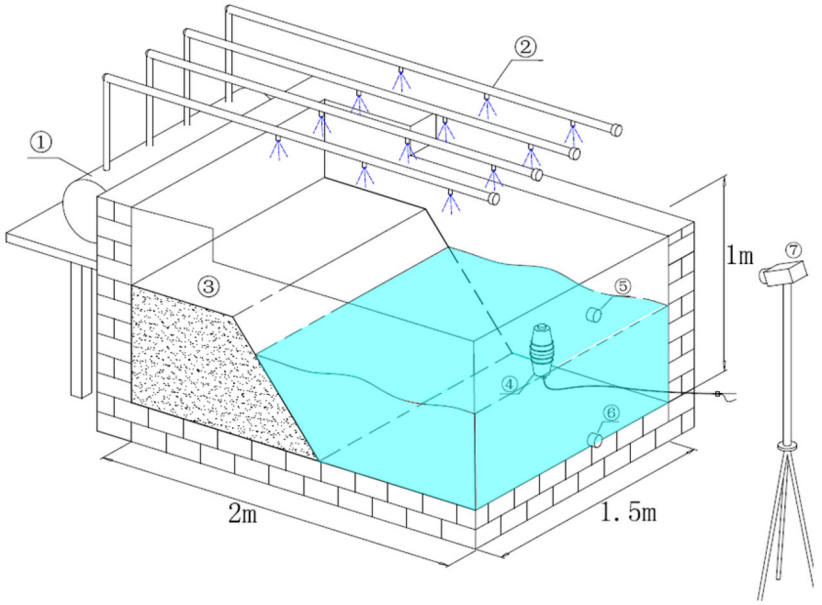

① water storage tank; ② spray nozzles; ③ bank slope model; ④ wave machine; ⑤ water inlet; ⑥ water outlet; ⑦ 3D laser scanner

Fig. 1 Three dimensional (3D) view of the physical simulation

Table 2 Scaling and computing method of test model

Factor	Slope height	Water level	Wave height	Slope angle	Density degree
Geological prototype	40–60 m	15–45 m	0.05–0.2 m	20–50°	0.30–0.89
Computing method of proportionality coefficient	$C_{\mathrm{l}} = \frac{l_{\mathrm{p}}}{l_{\mathrm{m}}} = 100$	$C_{\mathrm{H}} = \frac{H_{\mathrm{p}}}{H_{\mathrm{m}}} = 100$	$C_{\mathrm{h}} = \frac{h_{\mathrm{p}}}{h_{\mathrm{m}}} = 10$	$C_{\theta} = \frac{\theta_{\mathrm{p}}}{\theta_{\mathrm{m}}} = 1$	$C_{\mathrm{D}} = \frac{D_{\mathrm{p}}}{D_{\mathrm{m}}} = 1$
Model	0.4–0.6 m	0.15–0.45 m	0.005–0.02 m	20–50°	0.30–0.89

Experimental materials

The material composition of mountain reservoirs, which may include block stone, gravel, etc., is very complex. Being restricted by the experimental conditions of equipment size, load condition, and wave energy, these very large grain-size materials could not be tested within the flume; therefore, a similar material had to be considered in the indoor model test.

According to the Similarity Principle, the sizes of the prototype shape and the model shape must meet certain proportions, that is, the prototype size is reduced proportionately to the physical simulation experiment in the flume. Assuming that the volume of the slope prototype is V_{p}, the area of the prototype is S_{p}, the length of the prototype is l_{p}, and the slope angle of the prototype is θ_{p} and that the volume of the slope model is V_{m}, the area of the model is S_{m}, the length of model is l_{m}, and the slope angle of the model is θ_{m}, the similarity constant of each variable can be described as follows.

$$C_{\mathrm{l}} = \frac{l_{\mathrm{p}}}{l_{\mathrm{m}}},\ C_s = \frac{S_{\mathrm{p}}}{S_{\mathrm{m}}} = C_{\mathrm{l}}^2,\ C_{\mathrm{v}} = \frac{V_{\mathrm{p}}}{V_{\mathrm{m}}} = C_{\mathrm{l}}^3,\ C_{\theta} = \frac{\theta_{\mathrm{p}}}{\theta_{\mathrm{m}}} = 1$$

In this study, the model scale of the reservoir bank was 1:100, according to the test site, equipment, and test conditions, and the similarity coefficients of slope height (C_{l}), water level (C_{H}), slope angle (C_{θ}), and density degree (C_{D}) were confirmed according to Table 2. Then, the material size of the model test was obtained.

According to the aforementioned Similarity Principle, medium sand, fine sand, and silty soil were selected as the simulation materials (Table 3), and there was a portion of breccia and clay in the test material. For the medium sand, breccia with largest diameter of 2 mm accounted for about 20.8 % of the sediment, and clay particles less than 0.075 mm accounted for 1.7 % of the sediment. For the fine sand, a small portion of breccia with largest diameter of 2 mm accounted for about 7.4 % of the sediment, and clay particles less than 0.075 mm accounted for 7.4 % of it. For the silty soil, grains accounted for about 6.6 % of the sediment, particles 0.075–0.005 mm was 78.3 %, particles

Table 3 Material compositions and proportions in the model tests

Model material	Material composition and proportion						
	Material diameter (mm)	10–5 mm	5–2 mm	2–0.5 mm	0.5–0.25 mm	0.25–0.075 mm	0.075–0 mm
Medium sand	Proportion (%)	4.3 %	16.5 %	25.3 %	24.3 %	27.9 %	1.7 %
Fine sand	Proportion (%)	–	7.4 %	8.7 %	27.2 %	49.3 %	7.4 %
Silty soil	Proportion (%)	–	–	–	–	6.6 %	93.4 %

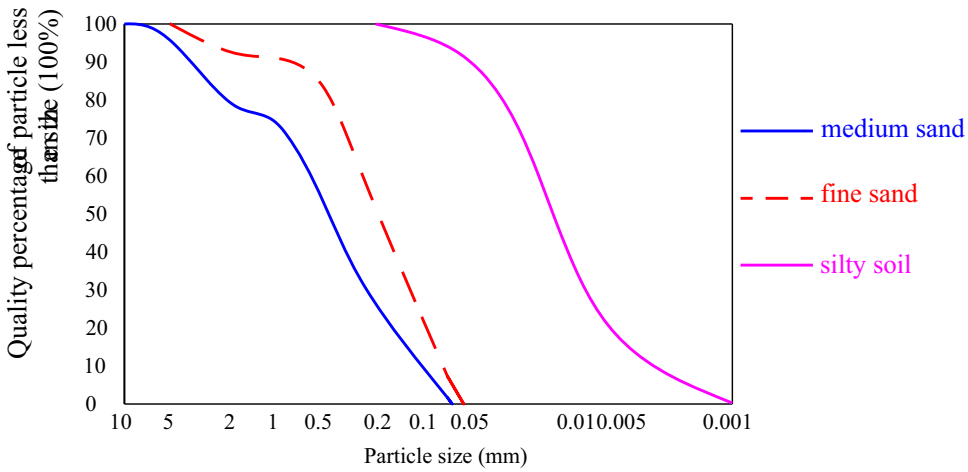

Fig. 2 Size distribution curves of the material compositions

<0.005 mm was 15.2 %, and there was a wave vibration response. Gradation curves for these materials are shown in Fig. 2.

Orthogonal experiment design

The orthogonal experiment design (OED) method is regarded as a modern approach for characterizing and optimizing system performance in many research areas. In general, practical engineering design and optimization usually involve three or more influential parameters that require full factorial design analysis. For a full factorial experiment of this study with four influential parameters (factors) and five levels, the number of necessary trials would be $5^4 = 625$. However, it is difficult and expensive to carry out such a large number of experiments. As an alternative, the OED method can be used to select representative points from the full factorial experiment in such a way that the points are distributed uniformly within the test range, and thus can adequately represent the overall situation. Table 3 summarizes the influence factors and level values selected in this study. The OED was also selected in this study.

We conducted 18 groups of orthogonal experiments in order to analyze the influences on BCW of material, bank slope, water level, wave height, and density degree. First, we established the basic characteristics of the model, width of 1.5 m, height of 0.45 m, and linear slope topography. Then, we adjusted the experiment model for other factors in accordance with Table 4.

Table 4 Design scheme of multi-factor orthogonal experiments

Serial number	Constrained material size (d_{60}) (mm)	Slope angle (°)	Water level (cm)	Wave height (cm)	Density degree
1	0.6	20	15	1.0	0.33
2	0.6	35	30	1.5	0.5
3	0.6	50	45	2.0	0.66
4	0.28	20	15	1.5	0.5
5	0.28	35	30	2.0	0.66
6	0.28	50	45	1.0	0.33
7	0.03	20	30	1.0	0.66
8	0.03	35	45	1.5	0.33
9	0.03	50	15	2.0	0.5
10	0.6	20	45	2.0	0.5
11	0.6	35	15	1.0	0.66
12	0.6	50	30	1.5	0.33
13	0.28	20	30	2.0	0.33
14	0.28	35	45	1.0	0.5
15	0.28	50	15	1.5	0.66
16	0.03	20	45	1.5	0.66
17	0.03	35	15	2.0	0.33
18	0.03	50	30	1.0	0.5

Fig. 3 Collapsed model in physical simulation flume

Fig. 4 ILRIS-3D scanner on tripod for different angles

For the OED method, the analysis of range (ANORA) was performed after collection of the experimental data. The ANORA assumes that, when analyzing the impact of a factor, the influences of other factors on the result are balanced, which means that the differences in levels of factor A are due to the factor itself. The ANOVA was used to estimate the relative significance of each parameter in terms of percentage contribution to the overall response.

Constrained material size d_{60} is a quantitative description of the experimental materials. In the paper, constrained material size d_{60} of silty soil, fine sand, and middle sand is 0.03 mm, 0.28 mm, and 0.6 mm, respectively.

Model design, data collection and processing

In the process of making the model, we first drew an outline on the flume according to the geometric model, and then prepared the soil samples with the designed contents. The particles were dried and sieved and mixed with fines, clay, and gravel. Then, an amount of water was supplied according to the desired initial water content, resulting in an initial water content of 16 %. The soil was mixed carefully with the water to ensure homogeneity of the soil. Then, a film was used to cover and seal the samples. After the soil was covered and sealed, it was stored for 24 h prior to the construction of the model. To build a slope model, the soil was compacted layer by layer with a layer thickness of 10 cm, and the model was made according to the preset geometry size. Finally, artificial waves were imposed on the slope until the bank model was destroyed (Fig. 3).

Regular measurement was performed during the test, and the slope phenomena of deformation and failure under

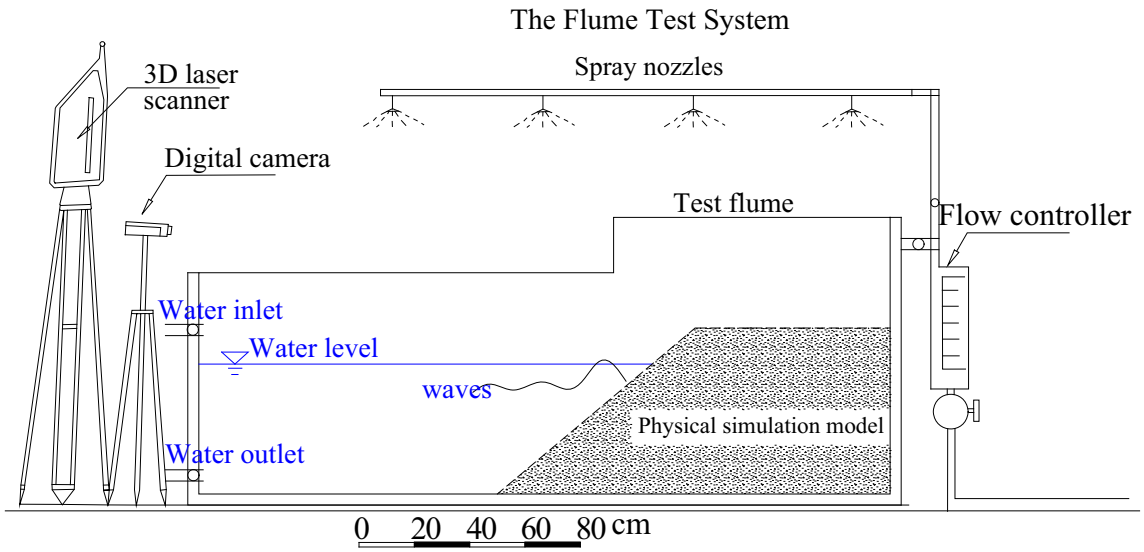

Fig. 5 Sketch of the test flume and its hydrological equipment

and over the water, the wave erosion belt width, and changes of the slope trailing edge were described. Three-dimensional (3D) laser scanning (model ILRIS-3D, Optech, Totonto, Canada), which enables surveyors to capture and define subjects point-by-point, was used (Fig. 4). The ILRIS-3D scanner system produces data that can be characterized as a point cloud, which is a large amount of data in a 3D coordinate system. In general, these data are defined by X, Y, and Z coordinates and are intended to be representative of the external surface of an object. Additionally, the spot spacing, the density of the scan, can be adjusted according to the application. A small value results in a high-resolution scan, and a large value results in a low-resolution scan. In this study, the spot spacing was set to 0.2 mm. The equipment allowed the model behavior to be investigated for different slope inclinations (Fig. 5).

As the number of experiments had been reduced greatly, the method of processing the orthogonal experimental data was very important. Range analysis (ANORA) is generally used in research to detect the most sensitive factor influencing a target index and verify its distinctiveness. In this study, range analysis was employed to discriminate the comparative significance of each factor, which was defined as the difference between the maximum and minimum value of the j-th factor, noted as R_j.

$$R_j = \max\{\overline{k}_{ji}\} - \min\{\overline{k}_{ji}\} \quad (1)$$

A larger R_j means a greater importance of the factor, and $\bar{k}_{ji}$ is the average targeting value of each experimental factor at the same level i in the orthogonal experiments, which was used to determine the optimal level and the optimal combination of factors. In our case, the lowest $\bar{k}_{ji}$ corresponded to the optimal level for each factor. $\bar{k}_{ji}$ was expressed as:

$$\bar{k}_{ji} = {}^{k_{ji}}\!/_{k_j}, \quad (2)$$

where the Arabic numerals i ($i = 1, 2, 3, 4$) are the level number and the j denotes a certain factor. k_{ji} is the sum of the targeting indexes of all levels in each factor j, and k_j is the total levels of the corresponding factor.

For example, the range R_j of the factor j is calculated via the following steps:

$$k_{j1} = M_{d1} + M_{d2} + M_{d3} + M_{d4} = 195.04$$

$$k_{j1} = M_{d5} + M_{d6} + M_{d7} + M_{d8} = 174.27$$

$$k_{j1} = M_{d9} + M_{d10} + M_{d11} + M_{d12} = 167.15$$

$$k_{j1} = M_{d13} + M_{d14} + M_{d15} + M_{d16} = 155.57$$

$$\bar{k}_{ji} = {}^{k_{ji}}\!/_{k_j} = \frac{195.04}{4} = 48.76$$

Table 5 Orthogonal experiment result of bank collapse

No.	Constrained material size (d_{60}) (mm)	Slope angle (°)	Water level (cm)	Wave height (cm)	Density degree	Width of bank collapse (cm)
1	0.6	20	15	1.0	0.33	3.40
2	0.6	35	30	1.5	0.5	14.3
3	0.6	50	45	2.0	0.66	13.2
4	0.28	20	15	1.5	0.5	7.8
5	0.28	35	30	2.0	0.66	6.5
6	0.28	50	45	1.0	0.33	15.9
7	0.03	20	30	1.0	0.66	1.41
8	0.03	35	45	1.5	0.33	7.7
9	0.03	50	15	2.0	0.5	14.3
10	0.6	20	45	2.0	0.5	6.9
11	0.6	35	15	1.0	0.66	8.4
12	0.6	50	30	1.5	0.33	26.1
13	0.28	20	30	2.0	0.33	10.1
14	0.28	35	45	1.0	0.5	2.3
15	0.28	50	15	1.5	0.66	11.2
16	0.03	20	45	1.5	0.66	0.8
17	0.03	35	15	2.0	0.33	10.7
18	0.03	50	30	1.0	0.5	8.0
K_{1j}[a]	12.08	5.08	7.84	6.59	12.34	
K_{2j}	8.98	8.34	9.32	10.30	8.95	
K_{3j}	7.18	14.81	11.08	11.34	6.94	

[a] K_{ij} is a statistical parameter of factor j in the level i

$\bar{k}_{ji} = 43.57; \bar{k}_{ji} = 41.79; \bar{k}_{ji} = 38.89;$

$R_j = \max\{\bar{k}_{ji}\} - \min\{\bar{k}_{ji}\} = 48.76 - 38.89 = 9.87$

where M_{di} is the bounded long wave (BLW) of the factor i. Other range values R_j of varying factors can be determined using the same calculation steps.

Results and discussion

According to the experiment scheme, we obtained BCW under different factors (Table 5).

Influence of slope angle on bank collapse

BCW showed a close relationship with the bank slope angle, and the characteristics of bank collapse under different slope angles are shown in Fig. 6. According to the figure, BCW increased gradually with an increase in slope angle. In addition, when the slope gradient was low, the bank collapse pattern was erosion type and the bank collapse width was small. When the bank slope gradient was larger, the bank collapse pattern is collapsed or slip type, and the width of bank collapse is larger. Further, we calculated many functions when fitting the test data (see Table 7), finally selecting the function with the highest correlation coefficient.

It is common knowledge that, the steeper the slope, the greater the sliding force along the potential sliding surface, making the stability coefficient of the slope relatively small. In this state, the bank is more prone to damage under the influence of wave and erosion, and the collapse scope is relatively large. Meanwhile, owing to the dynamic action of water, a gentle slope platform is formed near the water level, which is slower than the repose angle of the accumulation body underwater.

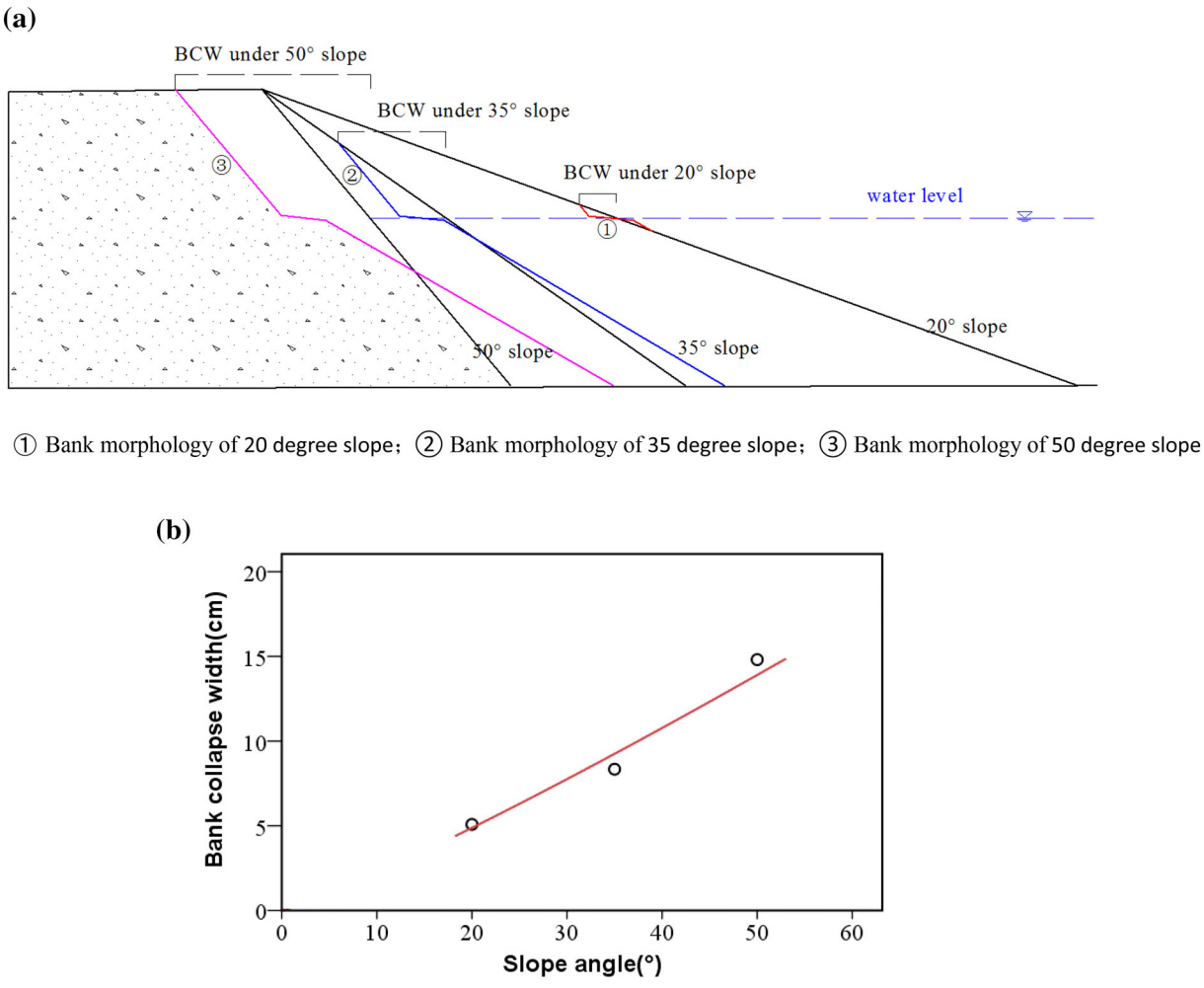

Fig. 6 Bank collapse width (BCW) under different slope angles. **a** Phenomena of bank model failure and accumulation. **b** Relation curve of BCW and slope angle, BCW is 5.08 cm, 8.34 cm, 14.81 cm, respectively, for which the fitting formula and correlation coefficient are $y = 0.0293\times^{1.7216}$ and $R^2 = 0.997$, respectively

Influence of material composition on bank collapse

BCW also showed a close relationship with model material. The characteristics of bank collapse under the different slope materials are shown in Fig. 7. According to the figure, the collapse width was largest for the medium sand bank and smallest for the silty soil bank.

It is common knowledge that, with less clay content and more sand content, the cohesive strength of the material is relatively small. During the fall of the water wave, the hydraulic gradient of sand slope is larger, which produces a dynamic water pressure on the slope. Therefore, the slope formed by the sand is more likely to be destroyed. However, when the clay content is relatively high, the permeability coefficient of the soil is relatively small, and wave energy along the inner slope is relatively weak, just carrying loose material on the slope surface, similar to peeling onions. Therefore, under the repeated erosion of the waves, the slope formed by the medium sand is most easily damaged, followed by the slope formed by fine sand, and then the silty soil slope, which yields the smallest collapse.

Influence of wave height on bank collapse

Wave erosion is an important external factor resulting in bank collapse, which is carried constantly toward the direction of the inner slope. According to the test results, BCW increased continuously with an increase in the wave height (Fig. 8). The effect of waves occurs in the aspects of scour of the slope and migration of the collapsed soil. As wave energy is directly proportional to the square of the wave height, higher wave height results in a nonlinear increase in the destructive power of the bank slope.

It is common knowledge that, the larger the wave, the faster its speed and the greater its energy, heightening the bank's risk of damage and increasing the carrying capacity of the surface soil. In addition, when the wave is higher, the

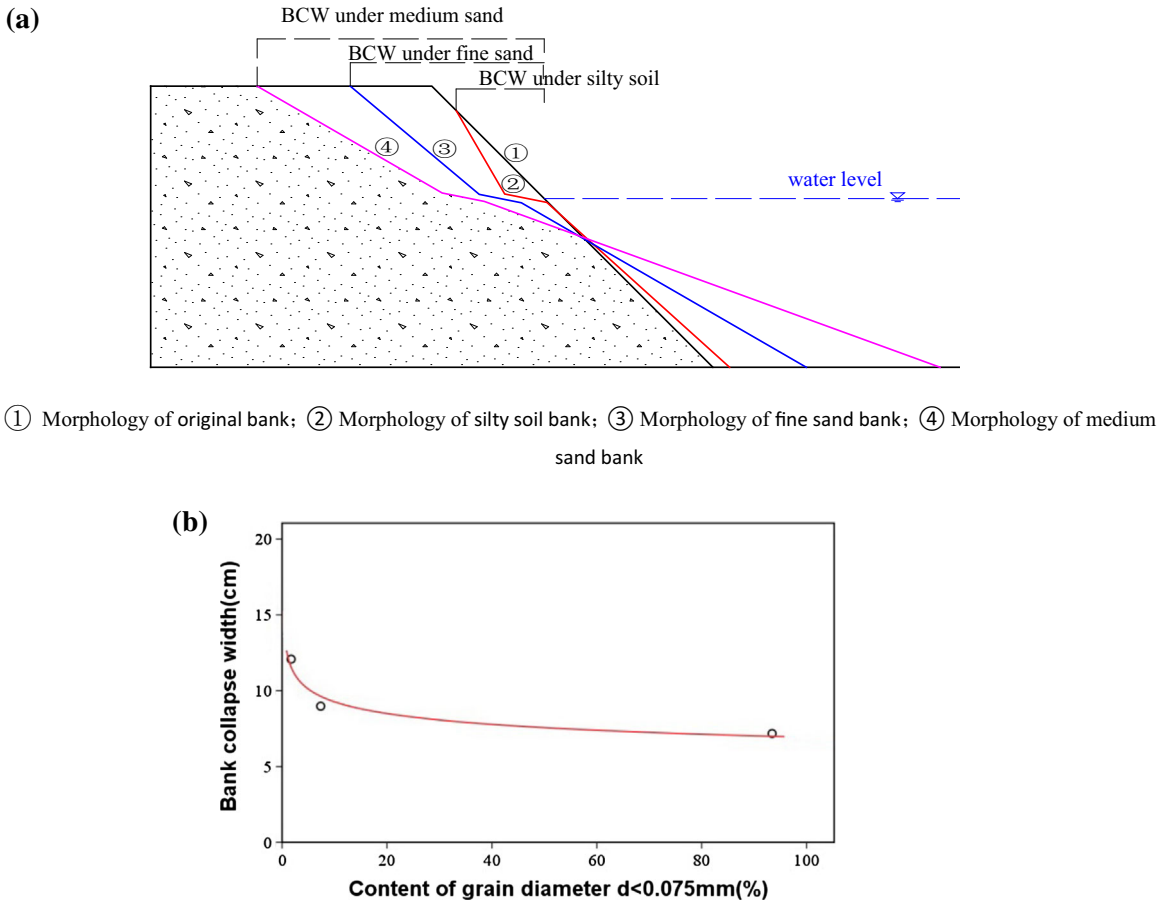

Fig. 7 BCW under different slope materials. **a** Phenomena of bank model failure and accumulation. **b** Relation curve of BCW and slope material, BCW is 7.18 cm, 8.98 cm,12.08 cm, respectively, for which the fitting formula and correlation coefficient are $y = 22.531\times^{-0.214}$ and $R^2 = 0.996$, respectively

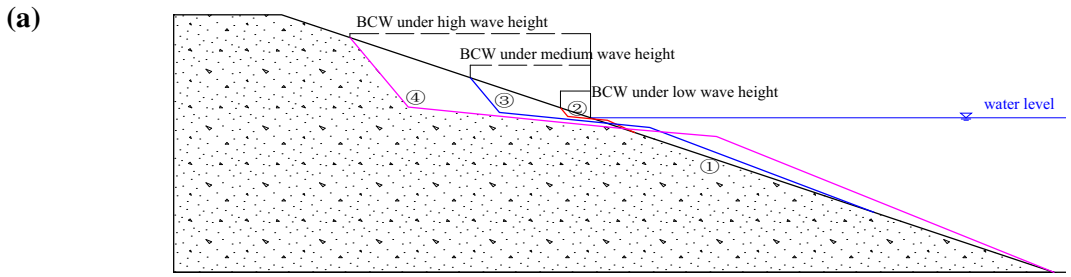

① Morphology of the original bank; ② Bank morphology for small wave height; ③ Bank morphology for medium wave height; ④ Bank morphology for high wave height.

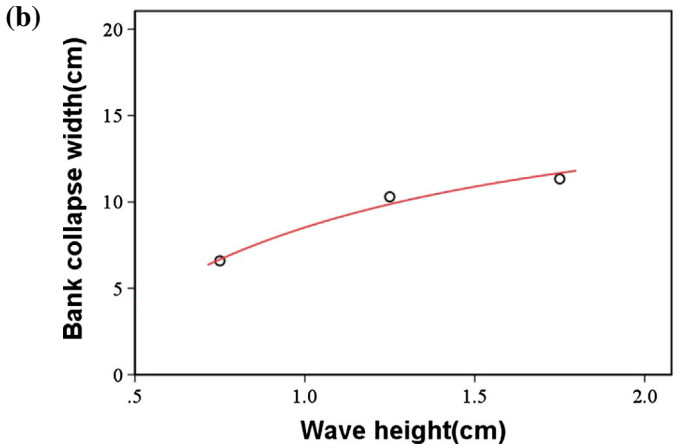

Fig. 8 BCW under different wave heights. **a** Phenomena of bank model failure and accumulation. **b** Relation curve of BCW and wave height, BCW is 6.59 cm, 10.30 cm, 11.34 cm respectively, for which the fitting formula and correlation coefficient are $y = e^{3.827-\frac{13.563}{x}}$ and $R^2 = 0.857$, respectively

water level of the slope is higher. During the course of the water level drop, the slope bears a larger hydraulic gradient, making it more likely to be destroyed. The combined effects of these two factors lead to the conclusion that the higher the wave height, the more probable the bank collapse.

Influence of water level on bank collapse

The characteristics of bank collapse under different water levels are shown in Fig. 9. The figure shows that BCW increased gradually with increase of water level. However, the range of increase of BCW was not very large. The collapsed soil had the effect of protecting the slope toe from further damage, and the slope morphology below and above the water level was linear. The slope angle above the water level was more than 5° higher than the slope angle beneath the water, and there was a platform near the water level.

It is common knowledge that, according to the repose angle theory, collapse will occur under water level above the reservoir water storage. The wider the range of the soil covered by water, the larger the range of unstable slope. In addition, no matter how high the water level, the slope angle under or above water is held constant.

Influence of density degree on bank collapse

In the orthogonal experiments, the parameter of density degree was used to describe the state of density of the different models. The characteristics of bank collapse under different density degree are shown in Fig. 10. The test results showed that the density degree had key effects on BCW and that BCW decreased with increasing density degree. The degree of bank collapse showed a significant difference under different conditions of density, with the BCW in the loose state being seven times that in the solid state.

It is common knowledge that, the higher the degree of the slope, the higher the soil strength. In the same wave action, the erosion resistance of soil with high density is greater. In addition, the permeability coefficient of the soil, the water head difference between the inside and outside of bank, and the dynamic water pressure are smaller.

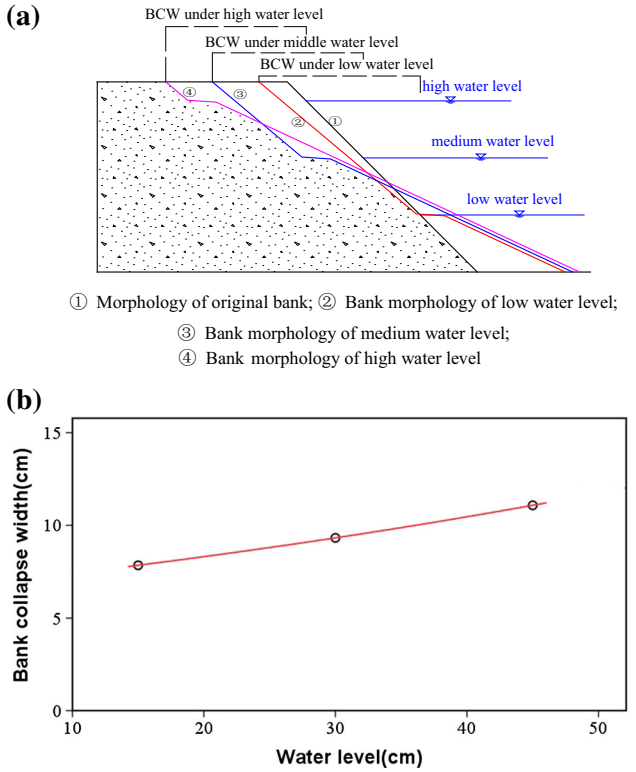

① Morphology of original bank; ② Bank morphology of low water level;
③ Bank morphology of medium water level;
④ Bank morphology of high water level

Fig. 9 Relation curve between BCW and water level. **a** Phenomenon of bank model failure and accumulation. **b** Relationship with fitting formula and correlation coefficient of $y = 15.483e^{-0.002\times}$ and $R^2 = 0.844$, respectively. Bank collapse width is 7.87 cm, 9.32 cm, 11.08 cm, respectively

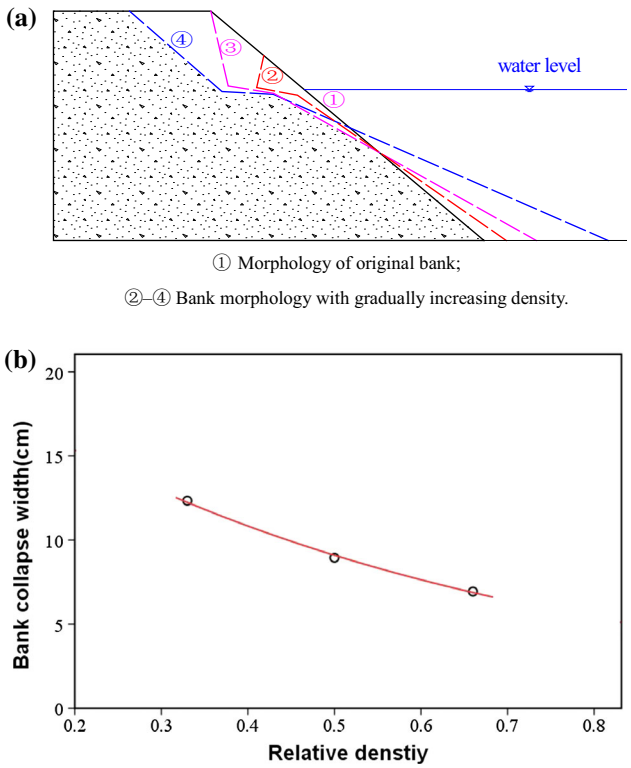

① Morphology of original bank;
②–④ Bank morphology with gradually increasing density.

Fig. 10 BCW under different density degrees. **a** Phenomena of bank model failure and accumulation. **b** Relationship with fitting formula and correlation coefficient of $y = 77.159e^{-2.886x}$ and $R^2 = 0.961$, respectively. BCW is 6.94 cm, 8.95 cm, 12.34 cm, respectively

Therefore, the stability of slope is improved with high-density soil. Owing to the combined effects of these two factors, the higher the density of the soil, the smaller the width of the bank collapse.

Statistical analysis

The width of bank collapse and the range analysis of the above experiments are shown in Table 6.

According to the results above, we were able to draw the following conclusions. First, the order of sensitivity was slope angle > density degree > material > wave height > water level, i.e., bank slope was the most significant factor among the influence factors of BCW, followed by density degree, material, wave height, and finally water level. Second, within the experiment factors, BCW was largest when the material was medium sand, when the slope angle was 50°, when the water level was 30 cm, and when the wave height was 1.5–2.0 cm. Thirdly, the change of BCW was relatively small with varying water level elevation.

In addition, a variety of different functions was used to fit the experimental results. Table 7 lists the correlation coefficient values of each equation type. The formula with the highest correlation was identified as the final fitting equation for each influencing factor.

According to the values of the correlation coefficients, which can be divided into three types, high (0.7–1), medium (0.3–0.7), and low (0–0.3) correlation coefficient, we can determine through the data above that the following factors are all highly related with BCW: slope angle, wave height, density degree, and material having particle size less than 0.075 mm. There was only a low relative relationship between BCW and water level. This result is the same as the sensitivity analysis of the various factors.

Based on the multi-factor orthogonal experiments, the multivariate regression method was used to establish the function of BCW with respect to the various factors (five main influence factors as the independent variables), and the established formula follows.

$$BCW = 2.5919e - 2.886d(0.4189X1 - 0.2554X2 + 0.3348X3 + 14.3529X4) \quad (3)$$

In the formula, BCW is bank collapse width (unit m), X_1 is slope angle (°), X_2 is water level (m), X_3 is wave height (cm), X_4 is d_{60} (mm), and d is relative density.

Table 6 Sensitivity of various factors on BCW[a]

Serial number	Factor	Amplitude of variation	Average width of bank collapse (m)	Range analysis	Order of sensitivity
1	Material	Medium sand	12.08×10^{-2}	4.90	Slope angle > density degree > material > wave height > water level
		Fine sand	8.98×10^{-2}		
		Silty soil	7.18×10^{-2}		
2	Slope angle	20°	5.08×10^{-2}	9.73	
		35°	8.34×10^{-2}		
		50°	14.81×10^{-2}		
3	Water level	0.15 m	7.84×10^{-2}	3.24	
		0.30 m	9.32×10^{-2}		
		0.45 m	11.08×10^{-2}		
4	Wave height	0.01 m	6.59×10^{-2}	4.75	
		0.015 m	10.30×10^{-2}		
		0.02 m	11.34×10^{-2}		
5	Density degree	0.33	12.34×10^{-2}	5.40	
		0.5	8.95×10^{-2}		
		0.66	6.94×10^{-2}		

[a] BCW was collected experimentally and processed statistically to calculate the range analysis according to Eqs. (1) and (2)

Table 7 Correlation coefficient of BCW and each factor

Factor	Linear type	Compound curve	Growth curve	Logarithmic curve	Sigmoid curve	Exponential curve	Inverse curve	Power curve	Logistic curve
Material size	0.780	0.871	0.871	0.916	0.837	0.871	0.916	0.997	0.871
Bank angle	0.976	0.996	0.996	0.922	0.969	0.996	0.850	0.996	0.996
Water level	0.844	0.844	0.844	0.815	0.855	0.844	0.815	0.829	0.844
Wave height	0.763	0.758	0.758	0.857	0.922	0.758	0.825	0.853	0.758
Density degree	0.923	0.934	0.955	0.910	0.912	0.961	0.833	0.912	0.934

Application condition

The model was obtained by a simulation test of coarse-grained soil in a mountain reservoir, so it is suitable for this type of bank slope. However, its usefulness to the plain reservoir still needs to be proved.

In addition, as a result of these tests, the mode of bank slope failure under the influence of water level fluctuation was determined and is shown in Fig. 11. Under the influence of water level fluctuation, the original bank was washed continuously until it produced a concave cavity, and soil collapsed and accumulated beneath the water. This process was repeated over and over again, a new concave cavity formed and the slope was destroyed further, until the length of the accumulated beach under the water was long and the angle of the bank was small enough so that the energy of waves transporting the soil was very weak. At this point, the bank slope was stable. It is worth noting that the bank collapse activity would likely develop again if one of the geological conditions or hydrological conditions changed.

Conclusions

An instrumented flume, designed and built at the State Key Laboratory of Geohazard Prevention and Geoenvironment Protection of China (SKLGP) was used successfully to study the degree of influence of each of several factors on bank slope collapse. A 3D laser scanner was used to evaluate the changes in topography, and a digital camera recorded all of the failure processes. For the BCW, we reached the following conclusions from the tests described above. The multi-factor model test indicated that the most sensitive factor affecting BCW is slope angle, followed by density degree, clay proportion, wave height, and water

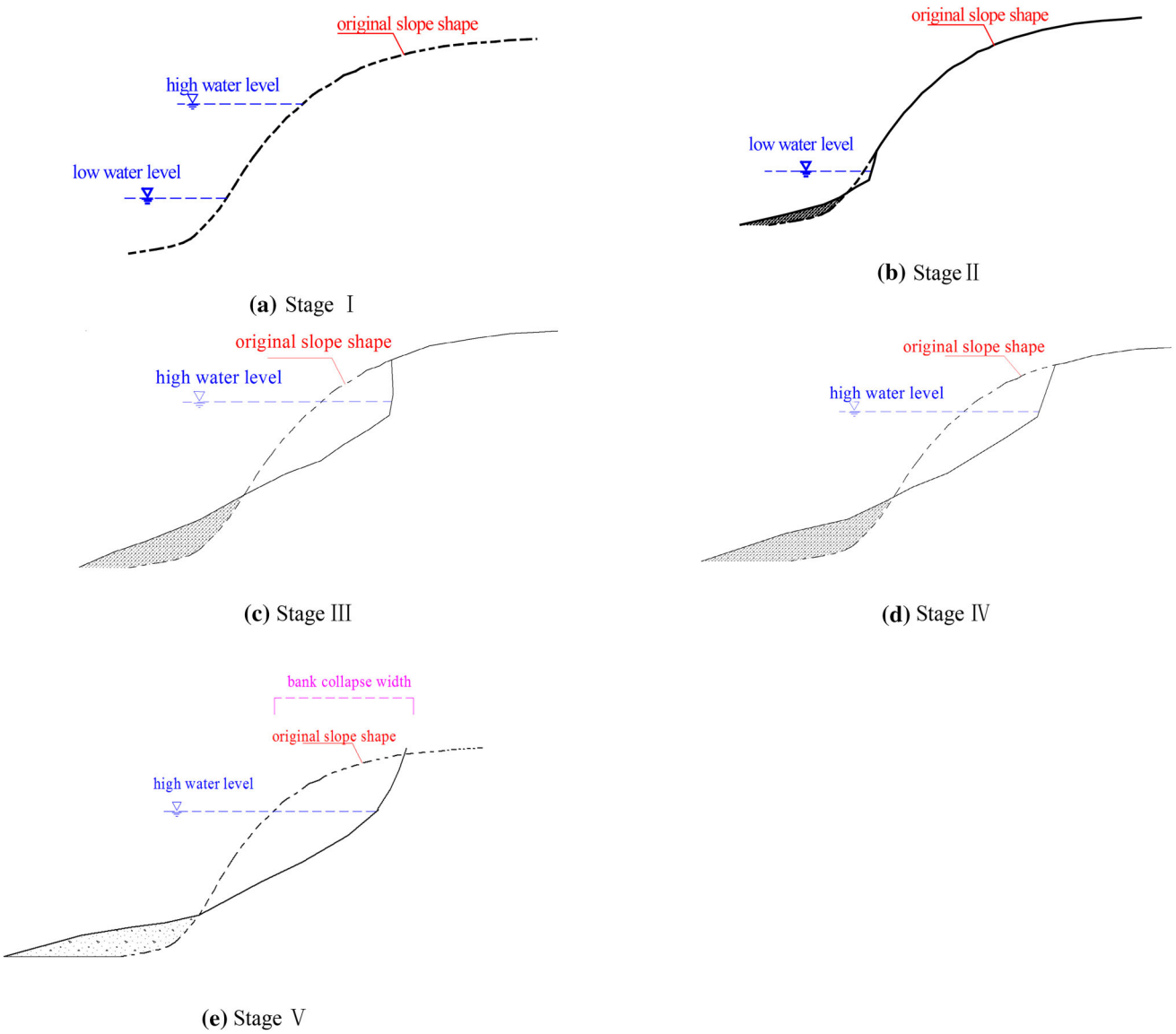

Fig. 11 Process of evolution of bank collapse width under reservoir water level. **a** The original bank. **b** During the reservoir water initial stage, the bank slope retreats due to collapse and a deposit forms at the slope toe. **c** When the storage level rises further, the scope of deposition in the toe slope increases gradually. **d** The bank above water level is stabilized gradually. **e** The eventual form of the bank slope, in which the slope reaches a stable state both under the water and above the water

level. When the slope angles above and below the water arrived at certain values, and the accumulated beach beneath the water was long enough, waves could no longer affect the erosion belt.

Acknowledgments We acknowledge support by the National Natural Science Foundation of China (No. 51308082), the Key Fund Project of the Sichuan Provincial Department of Education (No. 15ZA0075), and the Discovery Fund of the State Key Laboratory of Geohazard Prevention and Geoenvironment Protection (SKLGP 00002296), and the Talent Fund of Chengdu University of Technology (KYGG201303), China Postdoctoral Science Foundation (2013M540701). The authors are grateful to all of the technicians who worked in the laboratory of SKLGP for providing assistance throughout the experimental work, especially Dr. Dongpo Wang who provided advice on this research.

References

Andrew S, Andrea C, Stephen ED (2000) Bank and near-bank processes in an incised channel. J Geomorphol 35:193–217

Couper PR, Maddock IP (2001) Subaerial river bank erosion processes and their interaction with other bank erosion mechanisms on the River Arrow, Warwickshire, UK. J Earth Surf Process Landforms 26:631–646

Dapporto S, Rinaldi M, Casagli N (2003) Mechanisms of riverbank failure along the Arno River, central Italy. J Earth Surf Process Landforms 28:1303–1323

Fan YC, Zhang YY, Hu XW (2002) Prediction method and evaluation for reformation of reservoir bank (in Chinese). Sichuan W Power 21(4):69–83

Guan XY, Yang PL, Lv Y (2011) Relationships between soil particle size distribution and soil physical properties based on multifractal. Trans Chin Soc Agric Mach 42(3):44–51

Kachugin EG (1949) The reworking of banks in cases of river affluence, vol 24. USSR Academy of Sciences Publishers, Moscow

Kapayxev AB (1958) Rivers and reservoir dynamics. China Water, Beijing **(Chinese translation)**

Kondratjev NE (1956) Forecast dealing with bank reshaping in the area of water reservoir under the effect of wave action. Study of the State Hydrological Institute, Issue 56. Hydrometre, Leningrad

Ma SZI, Jia HB, Tang HM (2002) Analogy method with stable side shape to predict reservoir side rebuilding of rock shore (in Chinese). Earth Sci J China Univ Geo 27(2):231–234

Malik I, Matyja M (2008) Bank erosion history of a mountain stream determined by means of anatomical changes in exposed tree roots over the last 100 years (Bılá Opava River –Czech Republic). Geomorphology 98:126–142

Mosselman E, Shishikura T, Klaassen GJ (2000) Effect of bank stabilization on bend scour in anabranches of braided rivers. Phys Chem Earth (B) 25(7–8):699–704

Shu AP, Li FH, Yang K (2012) Bank-collapse disasters in the wide valley desert reach of the upper Yellow River. Procedia Environ Sci 13:2451–2457

Ta WQ, Xiao HL, Dong ZB (2008) Long-term morphodynamic changes of a desert reach of the Yellow River following upstream large reservoirs' operation. Geomorphology 7:249–259

Tang HM (2003) A study on reservoir bank collapse and its engineering prevention in the Three Gorges Project (in Chinese). J Ezhou Univ 10(4):1–6

Tang MG, Xu Q, Huang RQ (2006a) Types of typical bank slope collapses on the Three Gorges Reservoir (in Chinese). J Eng Geol 14(2):172–177

Tang MG, Xu Q, Huang RQ (2006b) Study on the forecasting parameters of bank collapse and influence factors in the Yangtze Three Gorges Project region (in Chinese). Chin J Chengdu Univ Techn (Science of Technology Edition) 33(5):460–464

Wang YM, Tang JH, Ling JM (2000) Study on prediction method for reservoir bank caving (in Chinese). Chin J Geotech Eng 22(5):569–571

Wu SB, Yu MH (2014) Experimental study on bank failure process and interaction with riverbed deformation due to fluvial hydraulic force. J Hydraul Eng 45(6):649–657

Xu RC (2003) Red stratum and dam (in Chinese). China University of Geosciences Press, Wuhan

Xu Q, Liu TX, Tang MG (2007) A new method of reservoir bank-collapse prediction in the Three Gorges Reservoir—River bank structure method (in Chinese). Hydrogeol Eng Geol 34(3):110–115

Yao ZY, Ta WQ, Jia XP, Xiao JH (2011) Riverbank erosion and accretion along the Ningxia-Inner Mongolia reaches of the Yellow River from 1958 to 2008. Geomorphol 127:99–106

Yin YP (2004) Prevention study on big geology hazards of new settlement address of three gorges (in Chinese). Geological Press, Beijing

Yu MH, Wei HY, Wu SB (2015) Experimental study on the bank erosion and interaction with near-bank bed evolution due to fluvial hydraulic force. Int J Sediment Res 01:81–89

Zhang QH, Ding XL, Zhang J (2002) A Study of slope rebuilding of the Fengjie stream segment after the Three Gorges Project reservoir impoundment (in Chinese). Chin J Rock Mech Eng 21(7):1007–1012